

Quark and lepton flavors with common modulus τ in A_4 modular symmetry

Hiroshi Okada ^{a,b*} and Morimitsu Tanimoto ^{c†}

^a*Asia Pacific Center for Theoretical Physics, Pohang 37673, Republic of Korea*

^b*Department of Physics, Pohang University of Science and Technology, Pohang 37673,
Republic of Korea*

^c*Department of Physics, Niigata University, Niigata 950-2181, Japan*

Abstract

We study quark and lepton mass matrices with the common modulus τ in the A_4 modular symmetry. The viable quark mass matrices are composed of modular forms of weights 2, 4 and 6. It is remarked that the modulus τ is close to i , which is a fixed point in the fundamental region of $SL(2, Z)$, and the CP symmetry is not violated. Indeed, the observed CP violation is reproduced at τ which is deviated a little bit from $\tau = i$. The charged lepton mass matrix is also given by using modular forms of weights 2, 4 and 6, where five cases have been examined. The neutrino mass matrix is generated in terms of the modular forms of weight 4 through the Weinberg operator. Lepton mass matrices are also consistent with the observed mixing angles at τ close to i for NH of neutrino masses. Allowed regions of τ of quarks and leptons overlap each other for all cases of the charged lepton mass matrix. However, the sum of neutrino masses is crucial to test the common τ for quarks and leptons. The minimal sum of neutrino masses $\sum m_i$ is 140meV at the common τ . The inverted hierarchy of neutrino masses is unfavorable in our framework. It is emphasized that our result suggests the residual symmetry $\mathbb{Z}_2^S = \{I, S\}$ in the quark and lepton mass matrices.

*E-mail address: hiroshi.okada@apctp.org

†E-mail address: tanimoto@muse.sc.niigata-u.ac.jp

1 Introduction

The origin of the flavors is one of important issues in particle physics. A lot of works have been presented by using the discrete groups for flavors to understand the flavor structures of quarks and leptons. In the early models of quark masses and mixing angles, the S_3 symmetry was used [1, 2]. It was also discussed to understand the large mixing angle [3] in the oscillation of atmospheric neutrinos [4]. For the last twenty years, the discrete symmetries of flavors have been developed, that is motivated by the precise observation of flavor mixing angles of leptons [5–14].

Many models have been proposed by using the non-Abelian discrete groups S_3 , A_4 , S_4 , A_5 and other groups with larger orders to explain the large neutrino mixing angles. Among them, the A_4 flavor model is attractive one because the A_4 group is the minimal one including a triplet irreducible representation, which allows for a natural explanation of the existence of three families of leptons [15–21]. However, variety of models is so wide that it is difficult to show a clear evidence of the A_4 flavor symmetry.

Recently, a new approach to the lepton flavor problem appeared based on the invariance of the modular group [22], where the model of the finite modular group $\Gamma_3 \simeq A_4$ has been presented. This work inspired further studies of the modular invariance to the lepton flavor problem. The modular group includes the finite groups S_3 , A_4 , S_4 , and A_5 [23]. Therefore, an interesting framework for the construction of flavor models has been put forward based on the $\Gamma_3 \simeq A_4$ modular group [22], and further, based on $\Gamma_2 \simeq S_3$ [24]. The flavor models have been proposed by using modular symmetries $\Gamma_4 \simeq S_4$ [25] and $\Gamma_5 \simeq A_5$ [26]. Phenomenological discussions of the neutrino flavor mixing have been done based on A_4 [27–29], S_4 [30–32], A_5 [33], and T' [34, 35] modular groups, respectively. In particular, the comprehensive analysis of the A_4 modular group has provided a distinct prediction of the neutrino mixing angles and the CP violating phase [28].

The A_4 modular symmetry has been also applied to the leptogenesis [36], on the other hand, it is discussed in the SU(5) grand unified theory (GUT) of quarks and leptons [37, 38]. The residual symmetry of the A_4 modular symmetry has presented the interesting phenomenology [39]. Furthermore, modular forms for $\Delta(96)$ and $\Delta(384)$ were constructed [40], and the extension of the traditional flavor group is discussed with modular symmetries [41]. The level 7 finite modular group $\Gamma_7 \simeq PSL(2, Z_7)$ is also presented for the lepton mixing [42]. Moreover, multiple modular symmetries are proposed as the origin of flavor [43]. The modular invariance has been also studied combining with the generalized CP symmetries for theories of flavors [44]. The quark mass matrix has been discussed in the S_3 and A_4 modular symmetries as well [45–47]. Besides mass matrices of quarks and leptons, related topics have been discussed in the baryon number violation [45], the dark matter [48, 49] and the modular symmetry anomaly [50]. Further phenomenology has been developed in many works [51–65] while theoretical investigations are also proceeded [66, 67].

In this work, we study both quarks and leptons in the A_4 modular symmetry. If the flavor of quarks and leptons is originated from a same two-dimensional compact space, quarks and leptons have same flavor symmetry and the common modulus τ . Therefore, it is challenging to reproduce observed hierarchical three Cabibbo-Kobayashi-Maskawa (CKM) mixing angles and the CP violating phase while observed large mixing angles are also reproduced in the lepton sector within the framework of the A_4 modular invariance with the common τ . This work provides a new aspect for the unification theory of the quark and lepton flavors. We have already discussed the quark mass matrices in the A_4 modular symmetry [45–47], where modular forms of weight 6 play an important role. In this paper, we present the comprehensive analysis by adopting modular forms of weight 4

and 6 in addition to modular forms of weight 2 for quarks and charged leptons. We take modular forms of weight 4 for the neutrino mass matrix generated by the Weinberg operator. We obtain the successful CKM mixing matrix at τ close to the fixed point i . We also discuss Pontecorvo-Maki-Nakagawa-Sakata (PMNS) mixing [68, 69] around $\tau = i$ as well as the CP violating Dirac phase of leptons which is expected to be observed at T2K and NO ν A experiments [70, 71], with reference to the sum of neutrino masses. It is found that the sum of neutrino masses is crucial to realize the common τ for quarks and leptons.

The paper is organized as follows. In section 2, we give a brief review on the modular symmetry and modular forms of weights 2, 4 and 6. In section 3, we present the model for quark mass matrices in the A_4 modular symmetry. In section 4, the modulus τ is fixed by the CKM matrix. In section 5, we discuss the lepton mass matrices, and in section 6, we examine τ in the lepton mixing and some predictions. Section 7 is devoted to a summary and discussions. In Appendix A, the tensor product of the A_4 group is presented. In Appendix B, we present how to obtain Dirac CP phase, Majorana phases and the effective mass of the $0\nu\beta\beta$ decay.

2 Modular group and modular forms

The modular group $\bar{\Gamma}$ is the group of linear fractional transformation γ acting on the modulus τ , belonging to the upper-half complex plane as:

$$\tau \longrightarrow \gamma\tau = \frac{a\tau + b}{c\tau + d}, \quad \text{where } a, b, c, d \in \mathbb{Z} \text{ and } ad - bc = 1, \quad \text{Im}[\tau] > 0, \quad (1)$$

which is isomorphic to $PSL(2, \mathbb{Z}) = SL(2, \mathbb{Z})/\{I, -I\}$ transformation. This modular transformation is generated by S and T ,

$$S : \tau \longrightarrow -\frac{1}{\tau}, \quad T : \tau \longrightarrow \tau + 1, \quad (2)$$

which satisfy the following algebraic relations,

$$S^2 = \mathbb{I}, \quad (ST)^3 = \mathbb{I}. \quad (3)$$

We introduce the series of groups $\Gamma(N)$ ($N = 1, 2, 3, \dots$), called principal congruence subgroups, defined by

$$\Gamma(N) = \left\{ \begin{pmatrix} a & b \\ c & d \end{pmatrix} \in SL(2, \mathbb{Z}), \quad \begin{pmatrix} a & b \\ c & d \end{pmatrix} = \begin{pmatrix} 1 & 0 \\ 0 & 1 \end{pmatrix} \pmod{N} \right\}. \quad (4)$$

For $N = 2$, we define $\bar{\Gamma}(2) \equiv \Gamma(2)/\{I, -I\}$. Since the element $-I$ does not belong to $\Gamma(N)$ for $N > 2$, we have $\bar{\Gamma}(N) = \Gamma(N)$. The quotient groups defined as $\Gamma_N \equiv \bar{\Gamma}/\bar{\Gamma}(N)$ are finite modular groups. In this finite groups Γ_N , $T^N = \mathbb{I}$ is imposed. The groups Γ_N with $N = 2, 3, 4, 5$ are isomorphic to S_3 , A_4 , S_4 and A_5 , respectively [23].

Modular forms of level N are holomorphic functions $f(\tau)$ transforming under the action of $\Gamma(N)$ as:

$$f(\gamma\tau) = (c\tau + d)^k f(\tau), \quad \gamma \in \Gamma(N), \quad (5)$$

where k is the so-called as the modular weight.

Superstring theory on the torus T^2 or orbifold T^2/Z_N has the modular symmetry [72–77]. Its low energy effective field theory is described in terms of supergravity theory, and string-derived supergravity theory has also the modular symmetry. Under the modular transformation of Eq.(1), chiral superfields $\phi^{(I)}$ transform as [78],

$$\phi^{(I)} \rightarrow (c\tau + d)^{-k_I} \rho^{(I)}(\gamma) \phi^{(I)}, \quad (6)$$

where $-k_I$ is the modular weight and $\rho^{(I)}(\gamma)$ denotes an unitary representation matrix of $\gamma \in \Gamma(N)$.

In the present article we study global supersymmetric models, e.g., minimal supersymmetric extensions of the Standard Model (MSSM). The superpotential which is built from matter fields and modular forms is assumed to be modular invariant, i.e., to have a vanishing modular weight. For given modular forms this can be achieved by assigning appropriate weights to the matter superfields.

The kinetic terms are derived from a Kähler potential. The Kähler potential of chiral matter fields $\phi^{(I)}$ with the modular weight $-k_I$ is given simply by

$$K^{\text{matter}} = \frac{1}{[i(\bar{\tau} - \tau)]^{k_I}} |\phi^{(I)}|^2, \quad (7)$$

where the superfield and its scalar component are denoted by the same letter, and $\bar{\tau} = \tau^*$ after taking the vacuum expectation value (VEV). Therefore, the canonical form of the kinetic terms is obtained by the overall normalization of the quark and lepton mass matrices ¹.

For $\Gamma_3 \simeq A_4$, the dimension of the linear space $\mathcal{M}_k(\Gamma_3)$ of modular forms of weight k is $k + 1$ [80–82], i.e., there are three linearly independent modular forms of the lowest non-trivial weight 2. These forms have been explicitly obtained [22] in terms of the Dedekind eta-function $\eta(\tau)$:

$$\eta(\tau) = q^{1/24} \prod_{n=1}^{\infty} (1 - q^n), \quad q = \exp(i2\pi\tau), \quad (8)$$

where $\eta(\tau)$ is a so called modular form of weight 1/2. In what follows we will use the following base of the A_4 generators S and T in the triplet representation:

$$S = \frac{1}{3} \begin{pmatrix} -1 & 2 & 2 \\ 2 & -1 & 2 \\ 2 & 2 & -1 \end{pmatrix}, \quad T = \begin{pmatrix} 1 & 0 & 0 \\ 0 & \omega & 0 \\ 0 & 0 & \omega^2 \end{pmatrix}, \quad (9)$$

where $\omega = \exp(i\frac{2}{3}\pi)$. The modular forms of weight 2 transforming as a triplet of A_4 can be written in terms of $\eta(\tau)$ and its derivative [22]:

$$\begin{aligned} Y_1(\tau) &= \frac{i}{2\pi} \left(\frac{\eta'(\tau/3)}{\eta(\tau/3)} + \frac{\eta'((\tau+1)/3)}{\eta((\tau+1)/3)} + \frac{\eta'((\tau+2)/3)}{\eta((\tau+2)/3)} - \frac{27\eta'(3\tau)}{\eta(3\tau)} \right), \\ Y_2(\tau) &= \frac{-i}{\pi} \left(\frac{\eta'(\tau/3)}{\eta(\tau/3)} + \omega^2 \frac{\eta'((\tau+1)/3)}{\eta((\tau+1)/3)} + \omega \frac{\eta'((\tau+2)/3)}{\eta((\tau+2)/3)} \right), \\ Y_3(\tau) &= \frac{-i}{\pi} \left(\frac{\eta'(\tau/3)}{\eta(\tau/3)} + \omega \frac{\eta'((\tau+1)/3)}{\eta((\tau+1)/3)} + \omega^2 \frac{\eta'((\tau+2)/3)}{\eta((\tau+2)/3)} \right), \end{aligned} \quad (10)$$

¹The most general Kähler potential consistent with the modular symmetry possibly contains additional terms, as recently pointed out in Ref. [79]. However, we consider only the simplest form of the Kähler potential.

which have the following q -expansions:

$$\mathbf{Y}_3^{(2)} = \begin{pmatrix} Y_1(\tau) \\ Y_2(\tau) \\ Y_3(\tau) \end{pmatrix} = \begin{pmatrix} 1 + 12q + 36q^2 + 12q^3 + \dots \\ -6q^{1/3}(1 + 7q + 8q^2 + \dots) \\ -18q^{2/3}(1 + 2q + 5q^2 + \dots) \end{pmatrix}. \quad (11)$$

They satisfy also the constraint [22]:

$$(Y_2(\tau))^2 + 2Y_1(\tau)Y_3(\tau) = 0. \quad (12)$$

The modular forms of the higher weight, k , can be obtained by the A_4 tensor products of the modular forms $\mathbf{Y}_3^{(2)}$, as given in Appendix A. For weight 4, that is $k = 4$, there are five modular forms by the tensor product of $\mathbf{3} \otimes \mathbf{3}$ as:

$$\mathbf{Y}_1^{(4)} = Y_1^2 + 2Y_2Y_3, \quad \mathbf{Y}_{1'}^{(4)} = Y_3^2 + 2Y_1Y_2, \quad \mathbf{Y}_{1''}^{(4)} = Y_2^2 + 2Y_1Y_3 = 0,$$

$$\mathbf{Y}_3^{(4)} = \begin{pmatrix} Y_1^{(4)} \\ Y_2^{(4)} \\ Y_3^{(4)} \end{pmatrix} = \begin{pmatrix} Y_1^2 - Y_2Y_3 \\ Y_3^2 - Y_1Y_2 \\ Y_2^2 - Y_1Y_3 \end{pmatrix}, \quad (13)$$

where $\mathbf{Y}_{1''}^{(4)}$ vanishes due to the constraint of Eq. (12). For wight 6, there are seven modular forms by the tensor products of A_4 as:

$$\mathbf{Y}_1^{(6)} = Y_1^3 + Y_2^3 + Y_3^3 - 3Y_1Y_2Y_3,$$

$$\mathbf{Y}_3^{(6)} \equiv \begin{pmatrix} Y_1^{(6)} \\ Y_2^{(6)} \\ Y_3^{(6)} \end{pmatrix} = \begin{pmatrix} Y_1^3 + 2Y_1Y_2Y_3 \\ Y_1^2Y_2 + 2Y_2^2Y_3 \\ Y_1^2Y_3 + 2Y_3^2Y_2 \end{pmatrix}, \quad \mathbf{Y}_{3'}^{(6)} \equiv \begin{pmatrix} Y_1'^{(6)} \\ Y_2'^{(6)} \\ Y_3'^{(6)} \end{pmatrix} = \begin{pmatrix} Y_3^3 + 2Y_1Y_2Y_3 \\ Y_3^2Y_1 + 2Y_1^2Y_2 \\ Y_3^2Y_2 + 2Y_2^2Y_1 \end{pmatrix}. \quad (14)$$

By using these modular forms of weights 2, 4, 6, we discuss quark and lepton mass matrices.

3 A_4 modular invariant quark mass matrices

Let us consider a A_4 modular invariant flavor model for quarks. There are freedoms for the assignments of irreducible representations and modular weights to quarks and Higgs doublets. The simplest one is to assign the triplet of the A_4 group to three left-handed quarks, but three different singlets ($\mathbf{1}, \mathbf{1}'', \mathbf{1}'$) of A_4 to the three right-handed quarks, (u^c, c^c, t^c) and (d^c, s^c, b^c) , respectively, where the sum of weights of the left-handed and the right-handed quarks is -2 .

Then, there appear three independent couplings in the superpotential of the up-type and down-type quark sectors, respectively, as follows:

$$w_u = \alpha_u u^c H_u \mathbf{Y}_3^{(2)} Q + \beta_u c^c H_u \mathbf{Y}_3^{(2)} Q + \gamma_u t^c H_u \mathbf{Y}_3^{(2)} Q, \quad (15)$$

$$w_d = \alpha_d d^c H_d \mathbf{Y}_3^{(2)} Q + \beta_d s^c H_d \mathbf{Y}_3^{(2)} Q + \gamma_d b^c H_d \mathbf{Y}_3^{(2)} Q, \quad (16)$$

where Q is the left-handed A_4 triplet quarks, and H_q is the Higgs doublets. The parameters α_q , β_q , γ_q ($q = u, d$) are constant coefficients. Assign the left-handed A_4 triplet Q to (u_L, c_L, t_L) and (d_L, s_L, b_L) . By using the decomposition of the A_4 tensor product in Appendix A, the superpotentials in Eqs.(15) and (16) give the mass matrix of quarks, which is written in terms of modular forms of weight 2:

$$M_q = v_q \begin{pmatrix} \alpha_q & 0 & 0 \\ 0 & \beta_q & 0 \\ 0 & 0 & \gamma_q \end{pmatrix} \begin{pmatrix} Y_1 & Y_3 & Y_2 \\ Y_2 & Y_1 & Y_3 \\ Y_3 & Y_2 & Y_1 \end{pmatrix}_{RL}, \quad (q = u, d), \quad (17)$$

where the argument τ in the modular forms $Y_i(\tau)$ is omitted. The coefficient v_q is the VEV of the Higgs field H_q . Unknown coefficients α_q , β_q , γ_q can be adjusted to the observed quark masses. The remained parameter is only the modulus, τ . The numerical study of the quark mass matrix in Eq.(17) is rather easy. However, it is impossible to reproduce observed hierarchical three CKM mixing angles by fixing one complex parameter τ .

	Q	(q_1^c, q_2^c, q_3^c)	H_q	$\mathbf{Y}_3^{(6)}, \mathbf{Y}_{3'}^{(6)}$	$\mathbf{Y}_3^{(4)}$	$\mathbf{Y}_3^{(2)}$
$SU(2)$	2	1	2	1	1	1
A_4	3	$(\mathbf{1}, \mathbf{1}'', \mathbf{1}')$	1	3	3	3
$-k_I$	-2	$(-4, -2, 0)$	0	$k = 6$	$k = 4$	$k = 2$

Table 1: Assignments of representations and weights $-k_I$ for MSSM fields and modular forms.

In order to obtain realistic quark mass matrices, we use modular forms of weight 4 and 6 in addition to weight 2 modular forms. They are given in Eqs.(13) and (14). We present the superpotential of the quark sector as follows:

$$w_q = \alpha_q q_1^c H_q \mathbf{Y}_3^{(6)} Q + \alpha'_q q_1^c H_q \mathbf{Y}_{3'}^{(6)} Q + \beta_q q_2^c H_q \mathbf{Y}_3^{(4)} Q + \gamma_q q_3^c H_q \mathbf{Y}_3^{(2)} Q, \quad (18)$$

where assignments of representations and weights for MSSM fields are given in Table 1. The quark mass matrix is written as:

$$M_q = \begin{pmatrix} \alpha_q & 0 & 0 \\ 0 & \beta_q & 0 \\ 0 & 0 & \gamma_q \end{pmatrix} \left[\begin{pmatrix} Y_1^{(6)} + g_q Y_1'^{(6)} & Y_3^{(6)} + g_q Y_3'^{(6)} & Y_2^{(6)} + g_q Y_2'^{(6)} \\ Y_2^{(4)} & Y_1^{(4)} & Y_3^{(4)} \\ Y_3^{(2)} & Y_2^{(2)} & Y_1^{(2)} \end{pmatrix} \right]_{RL}, \quad (19)$$

where $g_q \equiv \alpha'_q/\alpha_q$. Parameters α_q , β_q , γ_q are real, on the other hand, g_q are complex parameters. The parameters of our model are real six parameters, $\alpha_u, \beta_u, \gamma_u, \alpha_d, \beta_d, \gamma_d$, and complex parameters g_u, g_d in addition to the modulus τ . Now the model could be reconciled with observed values. Indeed, we have found parameter sets, which is consistent with the CKM observables and quark masses, in our numerical results.

4 Fixing modulus τ by the CKM mixing

In order to obtain the left-handed flavor mixing, we calculate $M_u^\dagger M_u$ and $M_d^\dagger M_d$, respectively. At first, we take a random point of τ and g_q which are scanned in the complex plane by generating

random numbers. The modulus τ is scanned in the fundamental region of the modular symmetry. In practice, the scanned range of $\text{Im}[\tau]$ is $[\sqrt{3}/2, 2]$, in which the lower-cut $\sqrt{3}/2$ is at the cusp of the fundamental region, and the upper-cut 2 is enough large for estimating Y_i . On the other hand, $\text{Re}[\tau]$ is scanned in the fundamental region $[-1/2, 1/2]$ of the modular group. We also scan in $|g_u| \in [0, 100]$ and $|g_d| \in [0, 100]$ while these phases are scanned in $[-\pi, \pi]$. Then, parameters $\alpha_q, \beta_q, \gamma_q$ ($q = u, d$) are given in terms of τ and g_q after inputting six quark masses.

Finally, we calculate three CKM mixing angles and the CP violating phase in terms of the model parameters τ, g_u and g_d . We keep the parameter sets, in which the value of each observable is reproduced within the three times of 1σ interval of error-bars. We continue this procedure to obtain enough points for plotting allowed region.

We input quark masses in order to constrain model parameters. Since the modulus τ obtains the expectation value by the breaking of the modular invariance at the high mass scale, the quark masses are put at the GUT scale. The observed masses and CKM parameters run to the GUT scale by the renormalization group equations (RGEs). In our work, we adopt numerical values of Yukawa couplings of quarks at the GUT scale 2×10^{16} GeV with $\tan\beta = 5$ in the framework of the minimal SUSY breaking scenarios [83, 84]:

$$\begin{aligned} y_d &= (4.81 \pm 1.06) \times 10^{-6}, & y_s &= (9.52 \pm 1.03) \times 10^{-5}, & y_b &= (6.95 \pm 0.175) \times 10^{-3}, \\ y_u &= (2.92 \pm 1.81) \times 10^{-6}, & y_c &= (1.43 \pm 0.100) \times 10^{-3}, & y_t &= 0.534 \pm 0.0341, \end{aligned} \quad (20)$$

which give quark masses as $m_q = y_q v_H$ with $v_H = 174$ GeV. In our numerical calculation, we input 2σ interval for quark masses.

We also use the following CKM mixing angles to focus on parameter regions consistent with the experimental data at the GUT scale 2×10^{16} GeV, where $\tan\beta = 5$ is taken [83, 84]:

$$\theta_{12} = 13.027^\circ \pm 0.0814^\circ, \quad \theta_{23} = 2.054^\circ \pm 0.384^\circ, \quad \theta_{13} = 0.1802^\circ \pm 0.0281^\circ. \quad (21)$$

Here θ_{ij} is given in the PDG notation of the CKM matrix V_{CKM} [85]. The observed CP violating phase is given as:

$$\delta_{CP} = 69.21^\circ \pm 6.19^\circ, \quad (22)$$

which is also in the PDG notation. The error intervals in Eqs. (20), (21) and (22) represent 1σ interval.

In our model, we have three complex parameters, τ, g_u and g_d after inputting six quark masses. The allowed regions of these parameters are obtained by inputting the observed three CKM mixing angles and CP violating phase with three times of 1σ interval in Eqs. (21) and (22). We have succeeded to reproduce completely four CKM elements in the parameter ranges of Table 2.

	$ \text{Re}[\tau] $	$\text{Im}[\tau]$	$ g_u $	$\text{Arg}[g_u]$	$ g_d $	$\text{Arg}[g_d]$
range	0 – 0.007	1.013 – 1.048	0 – 1.396	$[-\pi, \pi]$	0 – 1.443	$[-\pi, \pi]$

Table 2: Parameter ranges consistent with the observed CKM mixing angles and δ_{CP} .

As seen in Table 2, the modulus τ is close to i . The deviation from i is less than 5%. The modulus $\tau = i$ is a fixed point in the fundamental region of $\text{SL}(2, Z)$ under the transformation $S : \tau \rightarrow -1/\tau$. At $\tau = i$, CP is not violated as discussed in some works [41, 44, 86]. Indeed, we have succeeded to reproduce the observed CP violation at τ which is deviated a little bit from $\tau = i$.

In Fig. 1, we show the plot of $\text{Re}[\tau]$ and $\text{Im}[\tau]$, where output points are distributed overall in the 3σ range of the observed CKM elements, $|V_{us}|$, $|V_{cb}|$, $|V_{ub}|$ and δ_{CP} by choosing relevant g_u and g_d . It is noticed that $\text{Im}[\tau] = 1 - 1.013$ is excluded while $|\text{Re}[\tau]|$ is very small, less than 0.007.

The fixed point $\tau = i$ is realized if there is a residual symmetry $\mathbb{Z}_2^S = \{I, S\}$, which is the subgroup of A_4 . Then, the generator S commutes with $M_q^\dagger M_q$,

$$[M_q^\dagger M_q, S] = 0. \quad (23)$$

Therefore, the mass matrix is expected to be diagonal in the diagonal base \hat{S} . However, the eigenvalue -1 of S is degenerated, and so one pair off diagonal terms appear in $M_q^\dagger M_q$. We move to the diagonal base \hat{S} by a unitary transformation as: $\hat{S} = USU^\dagger$, while the quark mass matrix M_q is transformed as $M_q U^\dagger$. For the diagonal base $\hat{S} = \text{diag}(-1, -1, 1)$, the unitary matrix is given as:

$$U = \begin{pmatrix} \frac{2}{\sqrt{6}} & -\frac{1}{\sqrt{6}} & -\frac{1}{\sqrt{6}} \\ 0 & \frac{1}{\sqrt{2}} & \frac{1}{\sqrt{2}} \\ \frac{1}{\sqrt{3}} & \frac{1}{\sqrt{3}} & \frac{1}{\sqrt{3}} \end{pmatrix}. \quad (24)$$

Indeed, we have scanned model parameters around $\tau = i$ in the \hat{S} base since it is easy to find hierarchical quark mass matrices consistent with the observed CKM matrix.

We also show the allowed region of absolute values, $|g_u|$ and $|g_d|$ in Fig.2. It is remarked that the non-vanishing $|g_u|$ or $|g_d|$ is required to reproduce the CKM elements, however, those are at most of order 1. Indeed, the sum of $|g_u|$ and $|g_d|$ are larger than 0.25, but smaller than 2.3.

In Table 3, we show typical parameter sets and calculated CKM parameters. Ratios of α_q/γ_q and β_q/γ_q ($q = u, d$) correspond to the observed quark mass hierarchy. We also present the mixing matrices of up-type quarks and down-type quarks for the sample in Table 3 in order to investigate the flavor structure of each quark mass matrix. After moving to the diagonal basis of $\hat{S} = \text{diag}(-1, -1, 1)$ from the original one in Eq.(9), the mixing matrices of up- and down-quarks

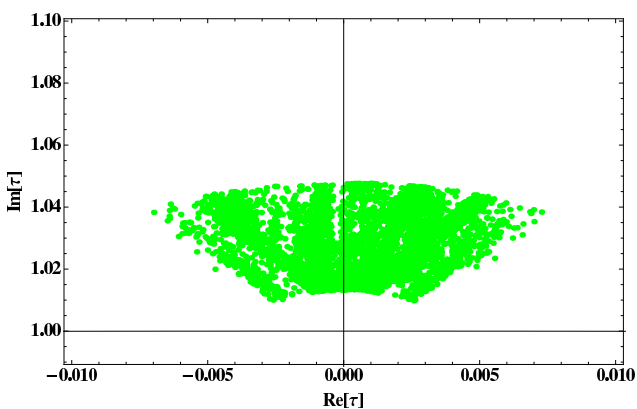


Figure 1: Allowed region on $\text{Re}[\tau]$ - $\text{Im}[\tau]$ plane consistent with three CKM mixing angles and δ_{CP} . The black curve is the boundary of the fundamental region, $|\tau| = 1$.

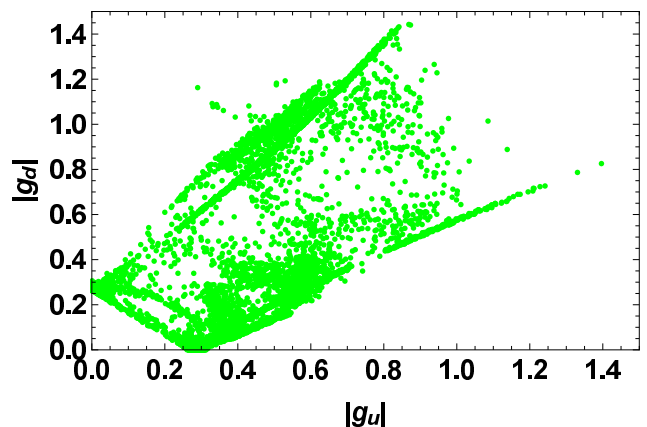


Figure 2: Allowed region on $|g_u|$ - $|g_d|$ plane consistent with three CKM mixing angles and δ_{CP} .

	A sample set
τ	$0.0007 + 1.041 i$
g_u	$0.407 - 0.198 i$
g_d	$0.745 + 0.176 i$
α_u/γ_u	1.74×10^2
β_u/γ_u	1.11×10^5
α_d/γ_d	1.88×10^1
β_d/γ_d	1.70×10^{-2}
$ V_{us} $	0.226
$ V_{cb} $	0.0487
$ V_{ub} $	0.0027
δ_{CP}	74.8°

Table 3: Numerical values of parameters and output of CKM parameters at a sample point.

are given as:

$$\begin{aligned}
V_u &\approx \begin{pmatrix} -0.529 & 0.848 & -0.025 \\ -0.820 - 0.200 i & -0.514 - 0.125 i & -0.091 \\ -0.089 - 0.017 i & -0.026 - 0.011 i & 0.995 - 0.016 i \end{pmatrix}, \\
V_d &\approx \begin{pmatrix} 0.067 & -0.645 & -0.761 \\ 0.067 & -0.752 + 0.101 i & 0.643 - 0.086 i \\ -0.995 - 0.016 i & -0.094 + 0.005 i & -0.008 - 0.006 i \end{pmatrix}.
\end{aligned} \tag{25}$$

The hierarchical flavor structure is partially seen as expected in the discussion of Eq.(24). After taking account of the degree of freedom of the permutation among A_4 triplet elements, (q_1, q_2, q_3) , we can obtain the observed CKM matrix $V_{\text{CKM}} = V_u^\dagger V_d$. Indeed, the permutation of (d_L, s_L, b_L) to (s_L, b_L, d_L) , which corresponds the exchange of columns $(1, 2, 3) \rightarrow (2, 3, 1)$ in V_d , gives the observed CKM matrix with keeping (u_L, c_L, t_L) .

In conclusion, our quark mass matrix with the A_4 modular symmetry can successfully reproduce the CKM mixing matrix completely. This successful result encourages us to investigate the lepton sector in the same framework. We discuss the lepton mass matrices with the A_4 modular symmetry in the next section.

5 Lepton mass matrix in the A_4 modular invariance

The modular A_4 invariance also gives the lepton mass matrix in terms of the modulus τ which is probably common both quarks and leptons if flavors of quarks and leptons are originated from a same two-dimensional compact space. The A_4 representations and weights are assigned for lepton fields relevantly as seen in Table 4, where the left-handed lepton doublets compose a A_4 triplet and the right-handed charged leptons are A_4 singlets. Weights of the left-handed leptons and the right-handed charged leptons are assigned like the quark ones in Table 4 (case I). In order to examine

the quantitative dependence of our result on weights of the right-handed charged leptons, we also consider other choices of weights for the right-handed ones as cases II – V of Table 4.

	L	(e^c, μ^c, τ^c)	H_u	H_d	$\mathbf{Y}_3^{(6)}, \mathbf{Y}_{3'}^{(6)}$	$\mathbf{Y}_3^{(4)}, \mathbf{Y}_1^{(4)}, \mathbf{Y}_{1'}$	$\mathbf{Y}_3^{(2)}$
$SU(2)$	2	1	2	2	1	1	1
A_4	3	(1, 1'', 1')	1	1	3	3, 1 1'	3
$-k_I$	-2	I: (-4, -2, 0) II: (-4, 0, 0) III: (0, 0, 0) IV: (-2, 0, 0) V: (-2, -2, -2)	0	0	$k = 6$	$k = 4$	$k = 2$

Table 4: Assignments of representations and weights $-k_I$ for MSSM fields and modular forms.

Assign the left-handed charged leptons a A_4 triplet $L = (e_L, \mu_L, \tau_L)$. Let us start with giving the charged lepton mass matrix M_E in terms of modular forms of weight 2, 4 and 6 in Eqs.(11), (13) and (14) as well as the quark sector. For the case I, it is presented as:

$$\text{I: } M_E = v_d \begin{pmatrix} \alpha_e & 0 & 0 \\ 0 & \beta_e & 0 \\ 0 & 0 & \gamma_e \end{pmatrix} \left[\begin{pmatrix} Y_1^{(6)} + g_e Y_1'^{(6)} & Y_3^{(6)} + g_e Y_3'^{(6)} & Y_2^{(6)} + g_e Y_2'^{(6)} \\ Y_2^{(4)} & Y_1^{(4)} & Y_3^{(4)} \\ Y_3^{(2)} & Y_2^{(2)} & Y_1^{(2)} \end{pmatrix} \right]_{RL}, \quad (26)$$

where coefficients α_e, β_e and γ_e are real parameters while g_e is complex one. For the case II, it is given as

$$\text{II: } M_E = v_d \begin{pmatrix} \alpha_e & 0 & 0 \\ 0 & \beta_e & 0 \\ 0 & 0 & \gamma_e \end{pmatrix} \left[\begin{pmatrix} Y_1^{(6)} + g_e Y_1'^{(6)} & Y_3^{(6)} + g_e Y_3'^{(6)} & Y_2^{(6)} + g_e Y_2'^{(6)} \\ Y_2^{(2)} & Y_1^{(2)} & Y_3^{(2)} \\ Y_3^{(2)} & Y_2^{(2)} & Y_1^{(2)} \end{pmatrix} \right]_{RL}. \quad (27)$$

On the other hand, a parameter g_e of the mass matrix disappears for cases III, IV and V. They are

$$\text{III: } M_E = v_d \begin{pmatrix} \alpha_e & 0 & 0 \\ 0 & \beta_e & 0 \\ 0 & 0 & \gamma_e \end{pmatrix} \left[\begin{pmatrix} Y_1^{(2)} & Y_3^{(2)} & Y_2^{(2)} \\ Y_2^{(2)} & Y_1^{(2)} & Y_3^{(2)} \\ Y_3^{(2)} & Y_2^{(2)} & Y_1^{(2)} \end{pmatrix} \right]_{RL}, \quad (28)$$

$$\text{IV: } M_E = v_d \begin{pmatrix} \alpha_e & 0 & 0 \\ 0 & \beta_e & 0 \\ 0 & 0 & \gamma_e \end{pmatrix} \left[\begin{pmatrix} Y_1^{(4)} & Y_3^{(4)} & Y_2^{(4)} \\ Y_2^{(2)} & Y_1^{(2)} & Y_3^{(2)} \\ Y_3^{(2)} & Y_2^{(2)} & Y_1^{(2)} \end{pmatrix} \right]_{RL}, \quad (29)$$

$$\text{V: } M_E = v_d \begin{pmatrix} \alpha_e & 0 & 0 \\ 0 & \beta_e & 0 \\ 0 & 0 & \gamma_e \end{pmatrix} \left[\begin{pmatrix} Y_1^{(4)} & Y_3^{(4)} & Y_2^{(4)} \\ Y_2^{(4)} & Y_1^{(4)} & Y_3^{(4)} \\ Y_3^{(4)} & Y_2^{(4)} & Y_1^{(4)} \end{pmatrix} \right]_{RL}, \quad (30)$$

respectively.

Suppose neutrinos to be Majorana particles. By using the Weinberg operator, the superpotential of the neutrino mass term, w_ν is given as:

$$w_\nu = -\frac{1}{\Lambda}(H_u H_u L L \mathbf{Y}_r^{(k)})_1, \quad (31)$$

where Λ is a relevant cut off scale and the A_4 singlet component is extracted. Since the left-handed lepton doublet has weight -2 , the superpotential is given in terms of modular forms of weight 4, $\mathbf{Y}_3^{(4)}$, $\mathbf{Y}_1^{(4)}$ and $\mathbf{Y}_{1'}^{(4)}$. By putting the vacuum expectation value of H_u (v_u) and taking $L = (\nu_e, \nu_\mu, \nu_\tau)$ for neutrinos, we have

$$\begin{aligned} w_\nu &= \frac{v_u^2}{\Lambda} \left[\begin{pmatrix} 2\nu_e\nu_e - \nu_\mu\nu_\tau - \nu_\tau\nu_\mu \\ 2\nu_\tau\nu_\tau - \nu_e\nu_\mu - \nu_\mu\nu_\tau \\ 2\nu_\mu\nu_\mu - \nu_\tau\nu_e - \nu_e\nu_\tau \end{pmatrix} \otimes \mathbf{Y}_3^{(4)} \right. \\ &\quad \left. + (\nu_e\nu_e + \nu_\mu\nu_\tau + \nu_\tau\nu_\mu) \otimes g_{\nu 1} \mathbf{Y}_1^{(4)} + (\nu_e\nu_\tau + \nu_\mu\nu_\mu + \nu_\tau\nu_e) \otimes g_{\nu 2} \mathbf{Y}_{1'}^{(4)} \right] \\ &= \frac{v_u^2}{\Lambda} \left[(2\nu_e\nu_e - \nu_\mu\nu_\tau - \nu_\tau\nu_\mu) Y_1^{(4)} + (2\nu_\tau\nu_\tau - \nu_e\nu_\mu - \nu_\mu\nu_e) Y_3^{(4)} + (2\nu_\mu\nu_\mu - \nu_\tau\nu_e - \nu_e\nu_\tau) Y_2^{(4)} \right. \\ &\quad \left. + (\nu_e\nu_e + \nu_\mu\nu_\tau + \nu_\tau\nu_\mu) g_{\nu 1} \mathbf{Y}_1^{(4)} + (\nu_e\nu_\tau + \nu_\mu\nu_\mu + \nu_\tau\nu_e) g_{\nu 2} \mathbf{Y}_{1'}^{(4)} \right], \quad (32) \end{aligned}$$

where $\mathbf{Y}_3^{(4)}$, $\mathbf{Y}_1^{(4)}$ and $\mathbf{Y}_{1'}^{(4)}$ are given in Eq. (13), and $g_{\nu 1}$, $g_{\nu 2}$ are complex parameters. The neutrino mass matrix is written as follows:

$$M_\nu = \frac{v_u^2}{\Lambda} \left[\begin{pmatrix} 2Y_1^{(4)} & -Y_3^{(4)} & -Y_2^{(4)} \\ -Y_3^{(4)} & 2Y_2^{(4)} & -Y_1^{(4)} \\ -Y_2^{(4)} & -Y_1^{(4)} & 2Y_3^{(4)} \end{pmatrix} + g_{\nu 1} \mathbf{Y}_1^{(4)} \begin{pmatrix} 1 & 0 & 0 \\ 0 & 0 & 1 \\ 0 & 1 & 0 \end{pmatrix} + g_{\nu 2} \mathbf{Y}_{1'}^{(4)} \begin{pmatrix} 0 & 0 & 1 \\ 0 & 1 & 0 \\ 1 & 0 & 0 \end{pmatrix} \right]_{LL}. \quad (33)$$

Model parameters for cases I and II are α_e , β_e , γ_e , g_e , $g_{\nu 1}$ and $g_{\nu 2}$ apart from the modulus τ while those of cases III, IV and V are α_e , β_e , γ_e , $g_{\nu 1}$ and $g_{\nu 2}$. Parameters α_e , β_e and γ_e are adjusted by the observed charged lepton masses. Therefore, the lepton mixing angles, the Dirac phase and Majorana phases are given by $g_{\nu 1}$, $g_{\nu 2}$ (g_e) in addition to the value of τ . Since τ is scanned around $\tau = i$, where the quark CKM matrix is reproduced, we expect to get some predictions in the lepton sector. Practically, we scan τ in the regions of $|\text{Re}[\tau]| \leq 0.1$ and $\text{Im}[\tau] \leq 1.12$, which is close to the one of the quark sector². Indeed, our predictions are almost unchanged even if the scanned region of $\text{Im}[\tau]$ is enlarged such as $\text{Im}[\tau] \leq 1.13$.

6 Modulus τ in the lepton mixing

We input charged lepton masses in order to constrain the model parameters. We take Yukawa couplings of charged leptons at the GUT scale 2×10^{16} GeV, where $\tan \beta = 5$ is taken as well as quark Yukawa couplings [83, 84]:

$$y_e = (1.97 \pm 0.024) \times 10^{-6}, \quad y_\mu = (4.16 \pm 0.050) \times 10^{-4}, \quad y_\tau = (7.07 \pm 0.073) \times 10^{-3}, \quad (34)$$

²If τ is scanned as a free parameter in the fundamental region, there may be other regions of τ which are consistent with observed lepton mixing angles.

observable	3σ range for NH	3σ range for IH
Δm_{atm}^2	$(2.436\text{--}2.618) \times 10^{-3} \text{ eV}^2$	$-(2.419\text{--}2.601) \times 10^{-3} \text{ eV}^2$
Δm_{sol}^2	$(6.79\text{--}8.01) \times 10^{-5} \text{ eV}^2$	$(6.79\text{--}8.01) \times 10^{-5} \text{ eV}^2$
$\sin^2 \theta_{23}$	0.433–0.609	0.436–0.610
$\sin^2 \theta_{12}$	0.275–0.350	0.275–0.350
$\sin^2 \theta_{13}$	0.02044–0.02435	0.02064–0.02457

Table 5: The 3σ ranges of neutrino parameters from NuFIT 4.1 for NH and IH [87].

where lepton masses are given by $m_\ell = y_\ell v_H$ with $v_H = 174$ GeV. We also use the following lepton mixing angles and neutrino mass parameters, which are given by NuFit 4.1 in Table 5 [87]. Since there are two possible spectrum of neutrinos masses m_i , which are the normal hierarchy (NH), $m_3 > m_2 > m_1$, and the inverted hierarchy (IH), $m_2 > m_1 > m_3$, we investigate both cases.

Neutrino masses and the PMNS matrix U_{PMNS} [68, 69] are obtained by diagonalizing $M_E^\dagger M_E$ and $M_\nu^* M_\nu$. We also investigate the sum of three neutrino masses $\sum m_i$ in our model since it is constrained by the recent cosmological data, [85, 88, 89]. The effective mass for the $0\nu\beta\beta$ decay is given as follows:

$$\langle m_{ee} \rangle = \left| m_1 c_{12}^2 c_{13}^2 + m_2 s_{12}^2 c_{13}^2 e^{i\alpha_{21}} + m_3 s_{13}^2 e^{i(\alpha_{31} - 2\delta_{CP}^\ell)} \right|, \quad (35)$$

where δ_{CP}^ℓ is the Dirac phase of leptons, and α_{21} , α_{31} are Majorana phases (see Appendix B).

Let us discuss numerical results for NH of neutrino masses in the case I of Eq.(26) like the quark sector. After inputting charged lepton masses, parameters τ , g_e , $g_{\nu 1}$ and $g_{\nu 2}$ are constrained by four observed quantities; three mixing angles of leptons and observed mass ratio $\Delta m_{\text{sol}}^2 / \Delta m_{\text{atm}}^2$.

At first, we show the allowed region on the $\text{Re}[\tau]$ – $\text{Im}[\tau]$ plane in Fig. 3. Observed three mixing angles of leptons are reproduced at cyan, blue and red points. At cyan points, the sum of neutrino masses is consistent with the cosmological upper-bound 120 meV. Red points denote common values of τ in both quarks and leptons. All allowed points are restricted in $\text{Im}[\tau] \leq 1.08$ and $|\text{Re}[\tau]| \leq 0.08$, that is around $\tau = i$. The red region does not satisfy $\sum m_i \leq 120\text{meV}$ unless it expands to $|\text{Re}[\tau]| \simeq 0.06$ or $\text{Im}[\tau] \simeq 1.07$. In the region of τ in Fig. 1, we discuss the neutrino masses and the CP violating phase δ_{CP}^ℓ .

We show the allowed region on the $\sum m_i$ – $\sin^2 \theta_{23}$ plane in Fig. 4, where colors (cyan, blue and red) of points correspond to points of τ in Fig. 3. The sum of neutrino masses is constrained by the cosmological upper-bound as seen in Fig. 4. The minimal cosmological model, $\Lambda\text{CDM} + \sum m_i$, provides a tight bound for the sum of neutrino masses, $\sum m_i < 120\text{meV}$ [88, 89] although it becomes weaker when the data are analysed in the context of extended cosmological models [85]. It is noticed that red points are in $\sum m_i \geq 190\text{meV}$ in Fig. 4. If these points will be completely excluded by the robust cosmological upper-bound of the sum of neutrino masses in the near future, the common region of τ between quarks and leptons vanishes. The calculated $\sin^2 \theta_{23}$ is distributed overall in the 3σ range of NuFIT 4.1 [87] below $\sum m_i = 120\text{meV}$.

We show the allowed region on the $\sum m_i$ – δ_{CP}^ℓ plane in Fig. 5. In the region of red points, δ_{CP}^ℓ is predicted to be in the restricted ranges, 60° – 120° and 240° – 300° . Below $\sum m_i = 120\text{meV}$ (cyan points), δ_{CP}^ℓ is allowed in $[0, 2\pi]$. In Fig. 6, we plot δ_{CP}^ℓ versus $\sin^2 \theta_{23}$ in order to see their

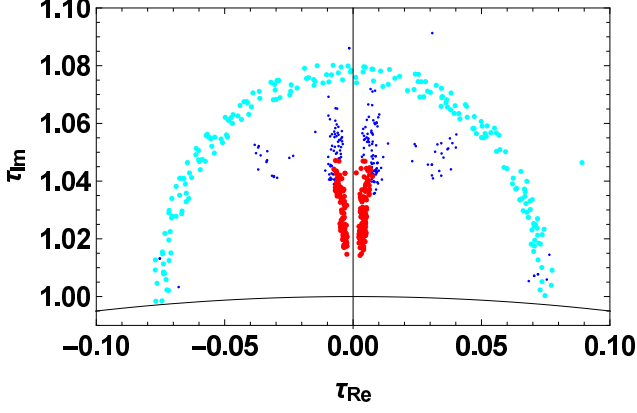


Figure 3: Allowed region on $\text{Re}[\tau]-\text{Im}[\tau]$ plane for NH in the case I of M_E . Observed mixing angles are reproduced at cyan, blue and red points. At cyan points, the sum of neutrino masses is below 120 meV. The solid curve is the boundary of the fundamental region, $|\tau| = 1$.

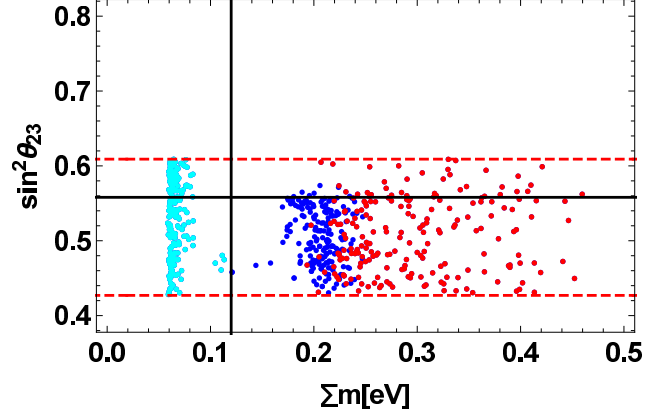


Figure 4: Allowed region on $\sum m_i-\sin^2\theta_{23}$ plane, where horizontal solid line denotes observed best-fit value, red dashed-lines denote the bound of 3σ interval, and vertical line is the cosmological bound, for NH in the case I of M_E . Color of points correspond to τ in Fig.3.

correlation. It is found that there is no distinct correlation between them. Around the best fit point of $\sin^2\theta_{23}$, the predicted δ_{CP}^ℓ is also in $[0, 2\pi]$ below $\sum m_i = 120$ meV (cyan points).

It is also noted that the effective mass of the $0\nu\beta\beta$ decay $\langle m_{ee} \rangle$ is predicted in 1.5–28 meV below $\sum m_i = 120$ meV.

In Table 6, we show a typical parameter set and the output of observables, which is chosen among cyan points (below $\sum m_i = 120$ meV). Ratios of α_e/γ_e and β_e/γ_e correspond to the observed charged lepton mass hierarchy.

As discussed in the quark sector, Eqs. (23) and (24), we have scanned model parameters around $\tau = i$ in the diagonal base of the generator S , where eigenvalues are $\text{diag}(1, -1, -1)$ in this case. The unitary matrix corresponding to Eq.(24) is obtained by its permutation of rows $1 \rightarrow 3 \rightarrow 2 \rightarrow 1$.

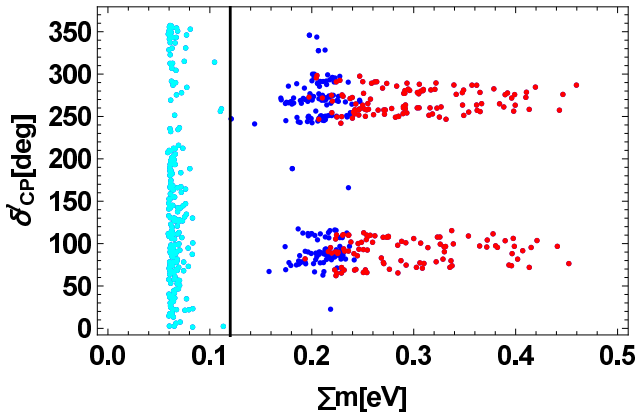


Figure 5: Allowed region on the $\sum m_i-\delta_{CP}^\ell$ plane, where the vertical line is the cosmological bound, for NH in the case I of M_E . Colors of points correspond to τ in Fig.3.

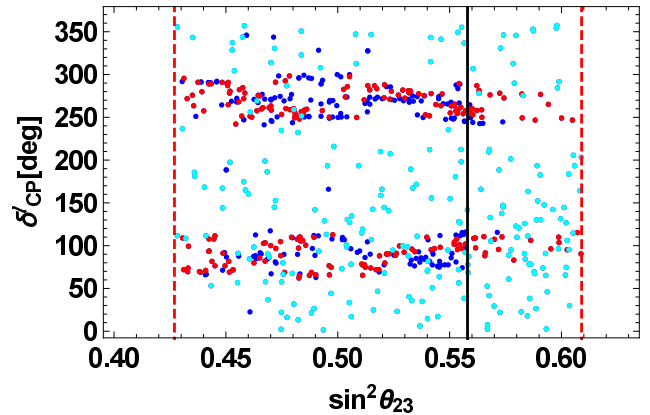


Figure 6: The correlation of $\sin^2\theta_{23}$ and δ_{CP}^ℓ , where the solid line denotes observed best-fit value and red dashed-lines denote the bound of 3σ interval, for NH in the case I of M_E .

	A sample set
τ	$0.028 + 1.075 i$
$g_{\nu 1}$	$-1.156 - 0.373 i$
$g_{\nu 2}$	$-0.617 - 0.441 i$
g_e	$-0.736 - 0.430 i$
α_e/γ_e	11.6
β_e/γ_e	3.92×10^{-3}
$\sin^2 \theta_{12}$	0.314
$\sin^2 \theta_{23}$	0.563
$\sin^2 \theta_{13}$	0.0233
δ_{CP}^ℓ	278°
$\sum m_i$	72.2 meV
$\langle m_{ee} \rangle$	8.0 meV

Table 6: Numerical values of parameters and output of PMNS parameters at a sample point.

Thanks to this base, it is easy to find hierarchical mixing matrices of the charged lepton. In this base, we present the mixing matrices of charged leptons and neutrinos for a sample of Table 6 as:

$$\begin{aligned}
U_\ell &\approx \begin{pmatrix} 0.627 + 0.759 i & -0.017 - 0.077 i & -0.159 - 0.005 i \\ -0.107 - 0.064 i & -0.560 + 0.237 i & -0.782 - 0.063 i \\ -0.108 - 0.064 i & 0.221 - 0.759 i & -0.404 + 0.444 i \end{pmatrix}, \\
U_\nu &\approx \begin{pmatrix} -0.101 - 0.856 i & -0.190 + 0.470 i & 0.008 - 0.001 i \\ -0.488 - 0.107 i & -0.640 - 0.557 i & -0.162 + 0.068 i \\ 0.078 + 0.035 i & 0.081 + 0.131 i & -0.978 + 0.116 i \end{pmatrix}.
\end{aligned} \tag{36}$$

The PMNS matrix is given by $U_{\text{PMNS}} = U_\ell^\dagger U_\nu$. It is noticed that the large θ_{23} comes from the charged lepton mass matrix while the large θ_{12} comes from the neutrino one.

In order to study the quantitative dependence of our result on weights of the right-handed charged leptons, we discuss other cases of those weights in Table 4, in which the mass matrix of the charged lepton is different from the quark one. Let us begin to examine the case II of Table 4, which presents the charged lepton mass matrix in Eq.(27). Indeed, we obtain the common region of τ for quarks and leptons in this case. Let us show the allowed region $\text{Re}[\tau]$ – $\text{Im}[\tau]$ plane in Fig. 7. Observed three mixing angles of leptons are reproduced at cyan, blue and red points. At cyan points, the sum of neutrino masses is below the cosmological upper-bound 120 meV. Red points denote common values of τ in both quarks and leptons. The red region does not satisfy $\sum m_i \leq 120\text{meV}$ unless it expands to $|\text{Re}[\tau]| \simeq 0.03$ and $\text{Im}[\tau] \simeq 1.06$.

We show the allowed region on the $\sum m_i$ – $\sin^2 \theta_{23}$ plane in Fig. 8, where colors (cyan, blue and red) of points correspond to points of τ in Fig. 8. The sum of neutrino masses is constrained by the cosmological upper-bound as seen in Fig. 7. It is noticed that red points are in $\sum m_i \geq 165\text{meV}$. If these points will be completely excluded by the robust cosmological upper-bound of the sum of neutrino masses in the near future, the common region of τ between quarks and leptons vanishes. Below $\sum m_i = 120\text{meV}$, $\sin^2 \theta_{23}$ is predicted in the range of 0.48–0.60.

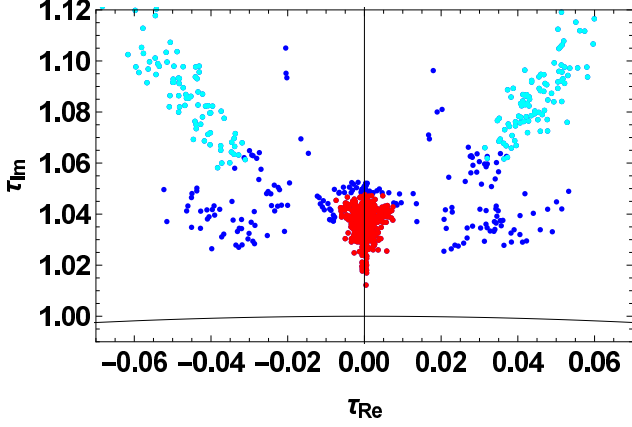


Figure 7: Allowed region on $\text{Re}[\tau]-\text{Im}[\tau]$ plane for NH in the case II of M_E . Observed mixing angles are reproduced at cyan, blue and red points. At cyan points, the sum of neutrino masses is below 120 meV. The solid curve is the boundary of the fundamental region, $|\tau| = 1$.

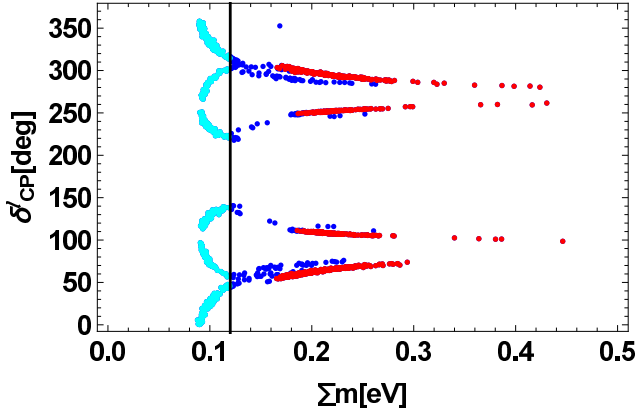


Figure 9: Allowed region on $\sum m_i-\delta_{CP}^\ell$ plane, where the vertical line is the cosmological bound, for NH in the case II of M_E . Colors of points correspond to τ in Fig.7.

We show the allowed region on the $\sum m_i-\delta_{CP}^\ell$ plane in Fig.9. In the region of red points, δ_{CP}^ℓ is predicted to be in the restricted ranges, $55^\circ-75^\circ$, $100^\circ-110^\circ$, $250^\circ-260^\circ$ and $285^\circ-305^\circ$. Below $\sum m_i = 120$ meV, δ_{CP}^ℓ is rather wide ranges in $0^\circ-100^\circ$, $110^\circ-135^\circ$, $225^\circ-250^\circ$ and $260^\circ-360^\circ$. We plot δ_{CP}^ℓ versus $\sin^2 \theta_{23}$ in Fig.10. It is found a clear correlation between them in contrast with the case I. At the best fit point of $\sin^2 \theta_{23}$, δ_{CP}^ℓ is predicted to be $0^\circ-20^\circ$ and $340^\circ-360^\circ$ below $\sum m_i = 120$ meV (cyan points).

We can also predict the effective mass of the $0\nu\beta\beta$ decay $\langle m_{ee} \rangle$. It is in 16–31 meV below $\sum m_i = 120$ meV.

As seen in the charged lepton mass matrix of Eqs. (26) and (27), there is a complex parameter g_e in addition to $g_{\nu 1}$ and $g_{\nu 2}$ of the neutrino sector for cases I and II. This additional parameter g_e gives the disadvantage to predict the CP violating phase. Indeed, δ_{CP}^ℓ is predicted in the wide

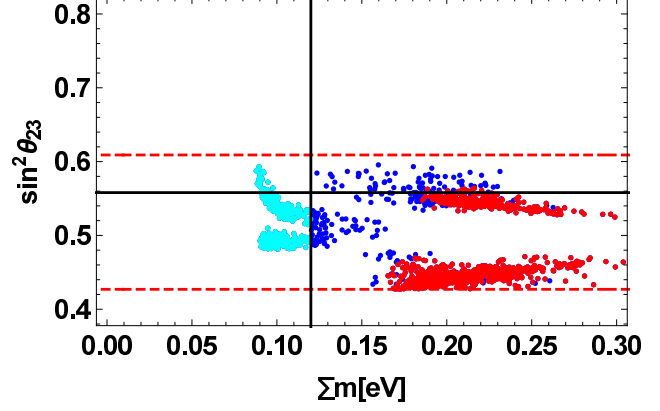


Figure 8: Allowed region on $\sum m_i-\sin^2 \theta_{23}$ plane, where horizontal solid line denotes observed best-fit one, red dashed-lines denote the bound of 3σ interval, and vertical line is the cosmological bound, for NH in the case II of M_E . Colors of points correspond to τ in Fig.7.

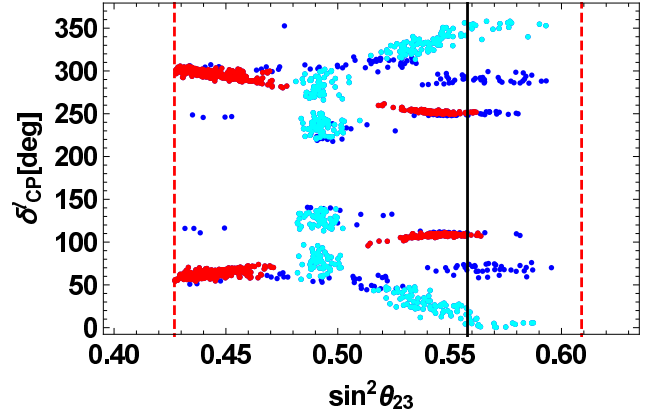


Figure 10: The correlation of $\sin^2 \theta_{23}$ and δ_{CP}^ℓ , where the solid line denotes observed best-fit value and red dashed-lines denote the bound of 3σ interval, for NH in the case II of M_E .

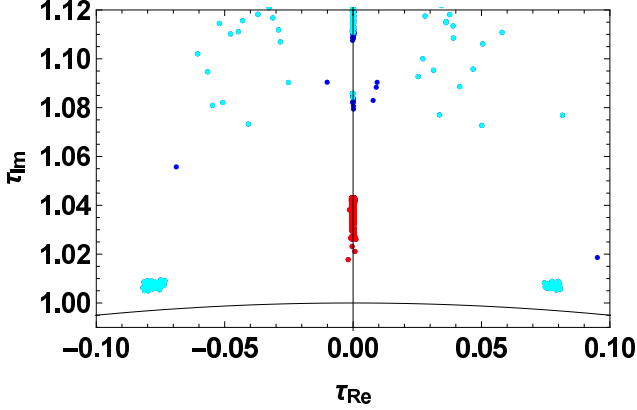


Figure 11: Allowed region on $\text{Re}[\tau]-\text{Im}[\tau]$ plane for NH in the case III of M_E . Observed mixing angles are reproduced at cyan, blue and red points. At cyan points, the sum of neutrino masses is below 120 meV. The solid curve is the boundary of the fundamental region, $|\tau| = 1$.

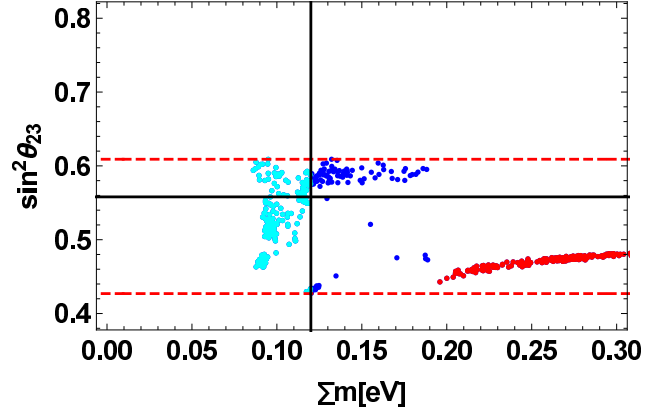


Figure 12: Allowed region on $\sum m_i - \sin^2 \theta_{23}$ plane, where horizontal solid line denotes observed best-fit one, red dashed-lines denote the bound of 3σ interval, and vertical line is the cosmological bound, for NH in the case III of M_E . Colors of points correspond to τ in Fig.11.

range for cases I and II as seen in Figs. 5 and 9. In order to improve the predictability of the model, cases III, IV and V provide attractive mass matrices³.

The mass matrix of Eq. (28) (case III) is the simplest one although this texture is excluded in the quark sector as discussed in Eq. (17). Remarkably, there exists a common region of τ for quarks and leptons in this case. Let us show the allowed region on the $\text{Re}[\tau]-\text{Im}[\tau]$ plane in Fig. 11. Observed three mixing angles of leptons are reproduced at cyan, blue and red points. The common region of τ in both quarks and leptons are presented by red points. At cyan points, the sum of neutrino masses is below the cosmological upper-bound 120 meV.

We show the allowed region on the $\sum m_i - \sin^2 \theta_{23}$ plane in Fig. 12, where colors (cyan, blue and red) of points correspond to points of τ in Fig. 11. It is found red points to be larger than $\sum m_i = 195 \text{ meV}$. The common region of τ in quarks and leptons vanishes if the cosmological upper-bound of the sum of neutrino masses is the robust one. Below $\sum m_i = 120 \text{ meV}$ (cyan points), $\sin^2 \theta_{23}$ is predicted in the range of 0.46–0.60.

We show the allowed region on the $\sum m_i - \delta_{CP}^\ell$ plane in Fig. 13. In the region of red points, δ_{CP}^ℓ is predicted to be in the restricted ranges, $70^\circ-90^\circ$ and $270^\circ-290^\circ$. However, below $\sum m_i = 120 \text{ meV}$, the predicted region of δ_{CP}^ℓ is expanded.

We plot δ_{CP}^ℓ versus $\sin^2 \theta_{23}$ in Fig. 14. It is found a clear correlation between them as well as the case II. At the best fit point of $\sin^2 \theta_{23}$, δ_{CP}^ℓ is predicted to be $110^\circ-125^\circ$ and $235^\circ-250^\circ$ below $\sum m_i = 120 \text{ meV}$ (cyan points), which is remarkably different from the ones in cases I and II. We can also predict the effective mass of the $0\nu\beta\beta$ decay $\langle m_{ee} \rangle$. It is in 15–30 meV below $\sum m_i = 120 \text{ meV}$.

For the case IV in Eq. (29), where the charged lepton mass matrix is composed of both weight 2 and 4 modular forms contrast to the case III, we obtain the common region of τ in quarks and leptons. Let us show the allowed region $\text{Re}[\tau]-\text{Im}[\tau]$ plane in Fig. 15. Observed three mixing angles

³These textures are not viable in the quark sector because only one complex parameter τ cannot reproduce observed four CKM elements.

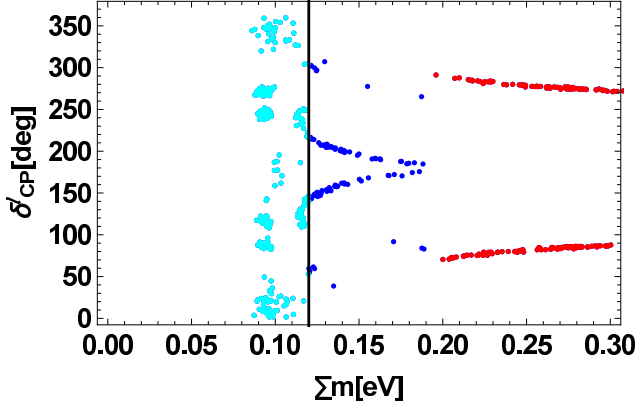


Figure 13: Allowed region on the $\sum m_i - \delta_{CP}^\ell$ plane, where the vertical line is the cosmological bound, for NH in the case III of M_E . Colors of points correspond to points of τ in Fig.11.

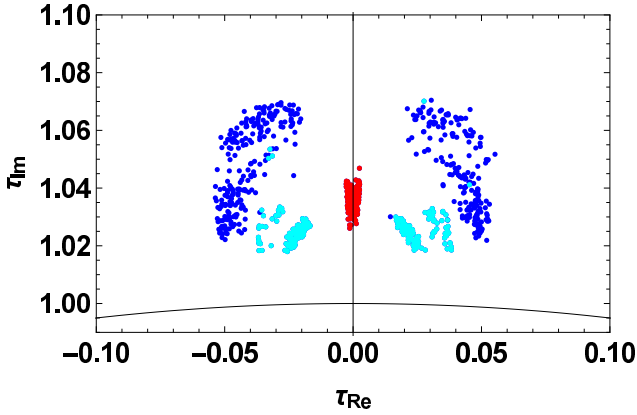


Figure 15: Allowed region on $\text{Re}[\tau] - \text{Im}[\tau]$ plane for NH in the case IV of M_E . Observed mixing angles are reproduced at cyan, blue and red points. At cyan points, the sum of neutrino masses is below 120 meV. The solid curve is the boundary of the fundamental region, $|\tau| = 1$.

of leptons are reproduced at cyan, blue and red points. At cyan points, the sum of neutrino masses is below the cosmological upper-bound 120 meV. Red points denote common values of τ in both quarks and leptons. As seen in Fig. 15, cyan points are not so far away from the red region.

We show the allowed region on the $\sum m_i - \sin^2 \theta_{23}$ plane in Fig. 16, where colors (cyan, blue and red) of points correspond to points of τ in Fig.15. It is found red points to be larger than $\sum m_i = 140\text{meV}$. The common region of τ in quarks and leptons vanishes under $\sum m_i = 120\text{meV}$. If the cosmological upper-bound of the sum of neutrino masses is allowed up to $\sum m_i = 160\text{meV}$ [85], $\sin^2 \theta_{23}$ is predicted to be 0.58–0.61 at the common τ of quarks and leptons.

We show the allowed region on the $\sum m_i - \delta_{CP}^\ell$ plane in Fig. 17. The predicted δ_{CP}^ℓ is in $150^\circ - 160^\circ$ and $200^\circ - 210^\circ$ at the common τ of quarks and leptons. However, below $\sum m_i = 120\text{meV}$, the

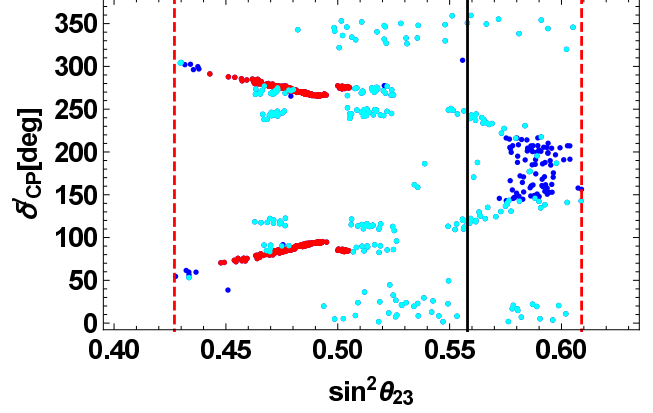


Figure 14: The correlation of $\sin^2 \theta_{23}$ and δ_{CP}^ℓ , where the black line denotes observed best-fit value and red dashed-lines denote the bound of 3σ interval, for NH in the case III of M_E .

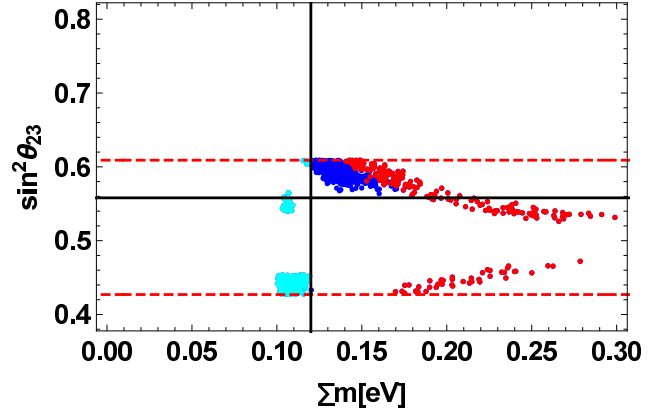


Figure 16: Allowed region on $\sum m_i - \sin^2 \theta_{23}$ plane, where horizontal solid line denotes observed best-fit value, dashed-lines denote the bound of 3σ interval, and vertical line is the cosmological bound, for NH in the case IV of M_E . Colors of points correspond to τ in Fig.15.

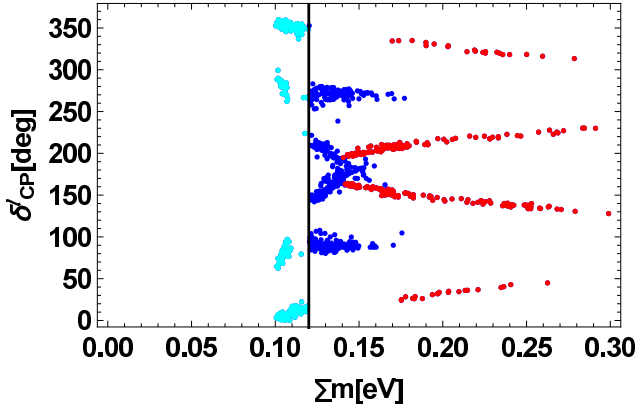


Figure 17: Allowed region on the $\sum m_i - \delta_{CP}^\ell$ plane, where the vertical line is the cosmological bound, for NH in the case IV of M_E . Colors of points correspond to τ in Fig.15.

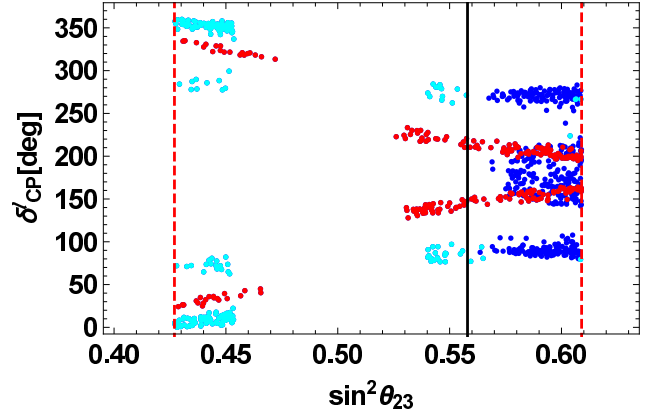


Figure 18: The correlation of $\sin^2 \theta_{23}$ and δ_{CP}^ℓ , where the solid line denotes observed best-fit value and red dashed-lines denote the bound of 3σ interval, for NH in the case IV of M_E .

predicted δ_{CP}^ℓ (cyan points) is $0^\circ-20^\circ$, $60^\circ-100^\circ$, $260^\circ-300^\circ$ and $340^\circ-360^\circ$.

We plot δ_{CP}^ℓ versus $\sin^2 \theta_{23}$ in Fig.18. It is found a clear correlation between them as well as cases II and III. At the best fit point of $\sin^2 \theta_{23}$, δ_{CP}^ℓ is predicted to be 90° and 270° below $\sum m_i = 120$ meV (cyan points).

Finally, the effective mass of the $0\nu\beta\beta$ decay $\langle m_{ee} \rangle$ is in 22–30 meV below $\sum m_i = 120$ meV.

For the case V in Eq.(30), where the charged lepton mass matrix is composed of only weight 4 modular forms, there is no common region of τ for quarks and leptons. Observed three mixing angles of leptons are not reproduced unless the sum of neutrino masses is larger than 450 meV, which is far away from the cosmological upper-bound 120 meV. Therefore, we omit to show numerical results for this case.

In Table 7, we summarize characteristic results of cases I–V including ones of IH. In our numerical calculations, we have not included the RGE effects in the lepton mixing angles and neutrino mass ratio $\Delta m_{sol}^2 / \Delta m_{atm}^2$. We suppose that those corrections are very small between the electroweak and GUT scales for NH of neutrino masses. This assumption is justified very well in the case of $\tan \beta \leq 5$ as far as the sum of neutrino masses is less than a few hundred meV [27, 90].

Finally, we discuss briefly the case of IH of neutrino masses. Indeed, there is the common region of τ in quarks and leptons for the case I of Eq.(26), where the predicted $\sin^2 \theta_{23}$ is larger than 0.6, and δ_{CP}^ℓ is around 70° and 290° . However, this case is completely excluded because the sum of neutrino masses is larger than 680 meV. Observed three mixing angles of leptons are not reproduced below $\sum m_i \leq 600$ meV. In the case II of Eq.(27), there is no common region of τ in quarks and leptons. Observed three mixing angles of leptons are not reproduced unless the sum of neutrino masses is larger than 200 meV. In the case III, it is found the common region of τ in quarks and leptons, but the sum of neutrino masses is larger than 420 meV. Observed three mixing angles of leptons are reproduced below $\sum m_i \leq 120$ meV, where $\sin^2 \theta_{23} \simeq 0.49-0.52$, $\delta_{CP}^\ell = 50^\circ-60^\circ$, $160^\circ-170^\circ$, $190^\circ-200^\circ$, $300^\circ-310^\circ$, and $\langle m_{ee} \rangle = 22-24$ meV. For cases IV and V, there are no common regions of τ in quarks and leptons. Below $\sum m_i \leq 120$ meV, observed three mixing angles of leptons are not reproduced in our scan regions of $|\text{Re}[\tau]| \leq 0.1$ and $\text{Im}[\tau] \leq 1.12$. In conclusion, IH of neutrino masses is unfavorable in our model. We summarize the results of IH in Table 7.

Cases		I	II	III	IV	V
common τ of quarks/leptons	NH	○	○	○	○	×
	IH	○	×	○	×	×
$\sum m_i$ at common τ	NH	≥ 190 meV	≥ 165 meV	≥ 195 meV	≥ 140 meV	—
	IH	≥ 680 meV	—	≥ 420 meV	—	—
δ_{CP}^ℓ at best fit of $\sin^2 \theta_{23}$ in $\sum m_i \leq 120$ meV	NH	0–360°	0–20°, 340°–360°	110°–125°, 235°–250°	0–20°, 340°–360°, 60°–100°, 260–300°	—
	IH	—	—	—	—	—
$\langle m_{ee} \rangle$ in $\sum m_i \leq 120$ meV	NH	1.5–28 meV	16–31 meV	15–30 meV	22–30 meV	—
	IH	—	—	22–24 meV	—	—

Table 7: Summary of characteristic predictions for NH and IH of cases I – V.

7 Summary and discussions

In this work, we have studied both quark and lepton mass matrices in the A_4 modular symmetry towards the unification of quark and lepton flavors. If flavors of quarks and leptons are originated from a same two-dimensional compact space, the quarks and leptons have same flavor symmetry and the common modulus τ .

The viable quark mass matrices are composed of modular forms of weights 2, 4 and 6. It is remarked that τ is close to i , which is a fixed point in the fundamental region of $SL(2, Z)$, and the CP symmetry is not violated. Indeed, we reproduce the observed CP violation of the quark sector at τ which is deviated a little bit from $\tau = i$.

The charged lepton mass matrix is also given by using modular forms of weights 2, 4 and 6. In order to study the quantitative dependence of our result on weights of the right-handed charged leptons, we have examined five cases I–V of them. The neutrino mass matrix is generated in terms of the modular forms of weight 4 through the Weinberg operator.

Our lepton mass matrices are also consistent with the observed mixing angles at τ close to i for NH of neutrino masses. It is found that allowed regions of τ of quarks and leptons overlap each other for all cases of the charged lepton mass matrix. The sum of neutrino masses is crucial to test the common τ for quarks and leptons. The predicted minimal sum of neutrino masses $\sum m_i$ is 140 meV at the common τ in the case IV. If the cosmological upper-bound of the sum of neutrino masses, 120 meV will be confirmed, the common region of τ of quarks and leptons vanishes. However, the allowed region of τ in both quark and lepton sectors could be shifted to a certain extent by some corrections such as the SUSY breaking effect through threshold corrections to masses and mixing angles. The appreciable shift of τ could be also occurred by the modification of the quark and lepton mass matrices. We need further investigation of the mass matrices to reproduce the observed CKM and PMNS on the common τ .

As well known, the modulus $\tau = i$ is a fixed point, which is invariant in the $\mathbb{Z}_2^S = \{I, S\}$ group. In our numerical results, the modulus τ is fixed close to $\tau = i$, which suggests the approximate residual symmetry in the quark and lepton mass matrices. Some corrections could violate the exact symmetry. The group theoretical investigation will be presented in the near future. It is also

emphasized that the spontaneous CP violation in Type IIB string theory is possibly realized nearby $\tau = i$, where the moduli stabilization as well as the calculation of Yukawa couplings is performed in a controlled way [91]. Thus, our phenomenological result of τ may be favored in the theoretical investigation.

It may be useful to note that IH of neutrino masses is unfavorable in our framework. Our study provides a phenomenological new aspect towards the unification of the quark and lepton flavors in terms of the modulus τ .

Acknowledgments

This research was supported by an appointment to the JRG Program at the APCTP through the Science and Technology Promotion Fund and Lottery Fund of the Korean Government. This was also supported by the Korean Local Governments - Gyeongsangbuk-do Province and Pohang City (H.O.). H. O. is sincerely grateful for the KIAS member.

Appendix

A Tensor product of A_4 group

We take the generators of A_4 group as follows:

$$S = \frac{1}{3} \begin{pmatrix} -1 & 2 & 2 \\ 2 & -1 & 2 \\ 2 & 2 & -1 \end{pmatrix}, \quad T = \begin{pmatrix} 1 & 0 & 0 \\ 0 & \omega & 0 \\ 0 & 0 & \omega^2 \end{pmatrix}, \quad (37)$$

where $\omega = e^{i\frac{2}{3}\pi}$ for a triplet. In this base, the multiplication rule of the A_4 triplet is

$$\begin{aligned} \begin{pmatrix} a_1 \\ a_2 \\ a_3 \end{pmatrix}_{\mathbf{3}} \otimes \begin{pmatrix} b_1 \\ b_2 \\ b_3 \end{pmatrix}_{\mathbf{3}} &= (a_1 b_1 + a_2 b_3 + a_3 b_2)_{\mathbf{1}} \oplus (a_3 b_3 + a_1 b_2 + a_2 b_1)_{\mathbf{1}'} \\ &\oplus (a_2 b_2 + a_1 b_3 + a_3 b_1)_{\mathbf{1}''} \\ &\oplus \frac{1}{3} \begin{pmatrix} 2a_1 b_1 - a_2 b_3 - a_3 b_2 \\ 2a_3 b_3 - a_1 b_2 - a_2 b_1 \\ 2a_2 b_2 - a_1 b_3 - a_3 b_1 \end{pmatrix}_{\mathbf{3}} \oplus \frac{1}{2} \begin{pmatrix} a_2 b_3 - a_3 b_2 \\ a_1 b_2 - a_2 b_1 \\ a_3 b_1 - a_1 b_3 \end{pmatrix}_{\mathbf{3}}, \end{aligned} \\ \mathbf{1} \otimes \mathbf{1} = \mathbf{1}, \quad \mathbf{1}' \otimes \mathbf{1}' = \mathbf{1}'' , \quad \mathbf{1}'' \otimes \mathbf{1}'' = \mathbf{1}' , \quad \mathbf{1}' \otimes \mathbf{1}'' = \mathbf{1} . \quad (38)$$

More details are shown in the review [6, 7].

B Majorana and Dirac phases and $\langle m_{ee} \rangle$ in $0\nu\beta\beta$ decay

Supposing neutrinos to be Majorana particles, the PMNS matrix U_{PMNS} [68, 69] is parametrized in terms of the three mixing angles θ_{ij} ($i, j = 1, 2, 3; i < j$), one CP violating Dirac phase δ_{CP} and

two Majorana phases α_{21} , α_{31} as follows:

$$U_{\text{PMNS}} = \begin{pmatrix} c_{12}c_{13} & s_{12}c_{13} & s_{13}e^{-i\delta_{\text{CP}}^\ell} \\ -s_{12}c_{23} - c_{12}s_{23}s_{13}e^{i\delta_{\text{CP}}^\ell} & c_{12}c_{23} - s_{12}s_{23}s_{13}e^{i\delta_{\text{CP}}^\ell} & s_{23}c_{13} \\ s_{12}s_{23} - c_{12}c_{23}s_{13}e^{i\delta_{\text{CP}}^\ell} & -c_{12}s_{23} - s_{12}c_{23}s_{13}e^{i\delta_{\text{CP}}^\ell} & c_{23}c_{13} \end{pmatrix} \begin{pmatrix} 1 & 0 & 0 \\ 0 & e^{i\frac{\alpha_{21}}{2}} & 0 \\ 0 & 0 & e^{i\frac{\alpha_{31}}{2}} \end{pmatrix}, \quad (39)$$

where c_{ij} and s_{ij} denote $\cos\theta_{ij}$ and $\sin\theta_{ij}$, respectively.

The rephasing invariant CP violating measure of leptons [92,93] is defined by the PMNS matrix elements $U_{\alpha i}$. It is written in terms of the mixing angles and the CP violating phase as:

$$J_{\text{CP}} = \text{Im} [U_{e1}U_{\mu 2}U_{e2}^*U_{\mu 1}^*] = s_{23}c_{23}s_{12}c_{12}s_{13}c_{13}^2 \sin \delta_{\text{CP}}^\ell, \quad (40)$$

where $U_{\alpha i}$ denotes the each component of the PMNS matrix.

There are also other invariants I_1 and I_2 associated with Majorana phases

$$I_1 = \text{Im} [U_{e1}^*U_{e2}] = c_{12}s_{12}c_{13}^2 \sin \left(\frac{\alpha_{21}}{2} \right), \quad I_2 = \text{Im} [U_{e1}^*U_{e3}] = c_{12}s_{13}c_{13} \sin \left(\frac{\alpha_{31}}{2} - \delta_{\text{CP}}^\ell \right). \quad (41)$$

We can calculate δ_{CP}^ℓ , α_{21} and α_{31} with these relations by taking account of

$$\begin{aligned} \cos \delta_{\text{CP}}^\ell &= \frac{|U_{\tau 1}|^2 - s_{12}^2 s_{23}^2 - c_{12}^2 c_{23}^2 s_{13}^2}{2c_{12}s_{12}c_{23}s_{23}s_{13}}, \\ \text{Re} [U_{e1}^*U_{e2}] &= c_{12}s_{12}c_{13}^2 \cos \left(\frac{\alpha_{21}}{2} \right), \quad \text{Re} [U_{e1}^*U_{e3}] = c_{12}s_{13}c_{13} \cos \left(\frac{\alpha_{31}}{2} - \delta_{\text{CP}}^\ell \right). \end{aligned} \quad (42)$$

In terms of these parametrization, the effective mass for the $0\nu\beta\beta$ decay is given as follows:

$$\langle m_{ee} \rangle = \left| m_1 c_{12}^2 c_{13}^2 + m_2 s_{12}^2 c_{13}^2 e^{i\alpha_{21}} + m_3 s_{13}^2 e^{i(\alpha_{31} - 2\delta_{\text{CP}}^\ell)} \right|. \quad (43)$$

References

- [1] S. Pakvasa and H. Sugawara, Phys. Lett. **73B** (1978) 61.
- [2] F. Wilczek and A. Zee, Phys. Lett. **70B** (1977) 418 Erratum: [Phys. Lett. **72B** (1978) 504].
- [3] M. Fukugita, M. Tanimoto and T. Yanagida, Phys. Rev. D **57** (1998) 4429 [hep-ph/9709388].
- [4] Y. Fukuda *et al.* [Super-Kamiokande Collaboration], Phys. Rev. Lett. **81** (1998) 1562 [hep-ex/9807003].
- [5] G. Altarelli and F. Feruglio, Rev. Mod. Phys. **82** (2010) 2701 [arXiv:1002.0211 [hep-ph]].
- [6] H. Ishimori, T. Kobayashi, H. Ohki, Y. Shimizu, H. Okada and M. Tanimoto, Prog. Theor. Phys. Suppl. **183** (2010) 1 [arXiv:1003.3552 [hep-th]].
- [7] H. Ishimori, T. Kobayashi, H. Ohki, H. Okada, Y. Shimizu and M. Tanimoto, Lect. Notes Phys. **858** (2012) 1, Springer.
- [8] D. Hernandez and A. Y. Smirnov, Phys. Rev. D **86** (2012) 053014 [arXiv:1204.0445 [hep-ph]].

- [9] S. F. King and C. Luhn, Rept. Prog. Phys. **76** (2013) 056201 [arXiv:1301.1340 [hep-ph]].
- [10] S. F. King, A. Merle, S. Morisi, Y. Shimizu and M. Tanimoto, New J. Phys. **16**, 045018 (2014) [arXiv:1402.4271 [hep-ph]].
- [11] M. Tanimoto, AIP Conf. Proc. **1666** (2015) 120002.
- [12] S. F. King, Prog. Part. Nucl. Phys. **94** (2017) 217 [arXiv:1701.04413 [hep-ph]].
- [13] S. T. Petcov, Eur. Phys. J. C **78** (2018) no.9, 709 [arXiv:1711.10806 [hep-ph]].
- [14] F. Feruglio and A. Romanino, arXiv:1912.06028 [hep-ph].
- [15] E. Ma and G. Rajasekaran, Phys. Rev. D **64**, 113012 (2001) [arXiv:hep-ph/0106291].
- [16] K. S. Babu, E. Ma and J. W. F. Valle, Phys. Lett. B **552**, 207 (2003) [arXiv:hep-ph/0206292].
- [17] G. Altarelli and F. Feruglio, Nucl. Phys. B **720** (2005) 64 [hep-ph/0504165].
- [18] G. Altarelli and F. Feruglio, Nucl. Phys. B **741** (2006) 215 [hep-ph/0512103].
- [19] Y. Shimizu, M. Tanimoto and A. Watanabe, Prog. Theor. Phys. **126** (2011) 81 [arXiv:1105.2929 [hep-ph]].
- [20] S. T. Petcov and A. V. Titov, Phys. Rev. D **97** (2018) no.11, 115045 [arXiv:1804.00182 [hep-ph]].
- [21] S. K. Kang, Y. Shimizu, K. Takagi, S. Takahashi and M. Tanimoto, PTEP **2018**, no. 8, 083B01 (2018) [arXiv:1804.10468 [hep-ph]].
- [22] F. Feruglio, doi:10.1142/9789813238053-0012 arXiv:1706.08749 [hep-ph].
- [23] R. de Adelhart Toorop, F. Feruglio and C. Hagedorn, Nucl. Phys. B **858**, 437 (2012) [arXiv:1112.1340 [hep-ph]].
- [24] T. Kobayashi, K. Tanaka and T. H. Tatsuishi, Phys. Rev. D **98** (2018) no.1, 016004 [arXiv:1803.10391 [hep-ph]].
- [25] J. T. Penedo and S. T. Petcov, Nucl. Phys. B **939** (2019) 292 [arXiv:1806.11040 [hep-ph]].
- [26] P. P. Novichkov, J. T. Penedo, S. T. Petcov and A. V. Titov, JHEP **1904** (2019) 174 [arXiv:1812.02158 [hep-ph]].
- [27] J. C. Criado and F. Feruglio, SciPost Phys. **5** (2018) no.5, 042 [arXiv:1807.01125 [hep-ph]].
- [28] T. Kobayashi, N. Omoto, Y. Shimizu, K. Takagi, M. Tanimoto and T. H. Tatsuishi, JHEP **1811** (2018) 196 [arXiv:1808.03012 [hep-ph]].
- [29] G. J. Ding, S. F. King and X. G. Liu, JHEP **1909** (2019) 074 [arXiv:1907.11714 [hep-ph]].
- [30] P. P. Novichkov, J. T. Penedo, S. T. Petcov and A. V. Titov, JHEP **1904** (2019) 005 [arXiv:1811.04933 [hep-ph]].

- [31] T. Kobayashi, Y. Shimizu, K. Takagi, M. Tanimoto and T. H. Tatsuishi, JHEP **02** (2020), 097 [arXiv:1907.09141 [hep-ph]].
- [32] X. Wang and S. Zhou, arXiv:1910.09473 [hep-ph].
- [33] G. J. Ding, S. F. King and X. G. Liu, Phys. Rev. D **100** (2019) no.11, 115005 [arXiv:1903.12588 [hep-ph]].
- [34] X. G. Liu and G. J. Ding, JHEP **1908** (2019) 134 [arXiv:1907.01488 [hep-ph]].
- [35] P. Chen, G. J. Ding, J. N. Lu and J. W. F. Valle, arXiv:2003.02734 [hep-ph].
- [36] T. Asaka, Y. Heo, T. H. Tatsuishi and T. Yoshida, JHEP **2001** (2020) 144 [arXiv:1909.06520 [hep-ph]].
- [37] F. J. de Anda, S. F. King and E. Perdomo, Phys. Rev. D **101** (2020) no.1, 015028 [arXiv:1812.05620 [hep-ph]].
- [38] T. Kobayashi, Y. Shimizu, K. Takagi, M. Tanimoto and T. H. Tatsuishi, arXiv:1906.10341 [hep-ph].
- [39] P. P. Novichkov, S. T. Petcov and M. Tanimoto, Phys. Lett. B **793** (2019) 247 [arXiv:1812.11289 [hep-ph]].
- [40] T. Kobayashi and S. Tamba, Phys. Rev. D **99** (2019) no.4, 046001 [arXiv:1811.11384 [hep-th]].
- [41] A. Baur, H. P. Nilles, A. Trautner and P. K. S. Vaudrevange, Phys. Lett. B **795** (2019) 7 [arXiv:1901.03251 [hep-th]].
- [42] G. Ding, S. F. King, C. Li and Y. Zhou, [arXiv:2004.12662 [hep-ph]].
- [43] I. de Medeiros Varzielas, S. F. King and Y. L. Zhou, Phys. Rev. D **101** (2020) no.5, 055033 [arXiv:1906.02208 [hep-ph]].
- [44] P. P. Novichkov, J. T. Penedo, S. T. Petcov and A. V. Titov, JHEP **1907** (2019) 165 [arXiv:1905.11970 [hep-ph]].
- [45] T. Kobayashi, Y. Shimizu, K. Takagi, M. Tanimoto, T. H. Tatsuishi and H. Uchida, Phys. Lett. B **794** (2019) 114 [arXiv:1812.11072 [hep-ph]].
- [46] H. Okada and M. Tanimoto, Phys. Lett. B **791** (2019) 54 [arXiv:1812.09677 [hep-ph]].
- [47] H. Okada and M. Tanimoto, arXiv:1905.13421 [hep-ph].
- [48] T. Nomura and H. Okada, Phys. Lett. B **797** (2019) 134799 [arXiv:1904.03937 [hep-ph]].
- [49] H. Okada and Y. Orikasa, arXiv:1907.04716 [hep-ph].
- [50] Y. Kariyazono, T. Kobayashi, S. Takada, S. Tamba and H. Uchida, Phys. Rev. D **100** (2019) no.4, 045014 [arXiv:1904.07546 [hep-th]].
- [51] T. Nomura and H. Okada, arXiv:1906.03927 [hep-ph].

- [52] H. Okada and Y. Orikasa, arXiv:1908.08409 [hep-ph].
- [53] T. Nomura, H. Okada and O. Popov, Phys. Lett. B **803** (2020) 135294 [arXiv:1908.07457 [hep-ph]].
- [54] J. C. Criado, F. Feruglio and S. J. D. King, JHEP **2002** (2020) 001 [arXiv:1908.11867 [hep-ph]].
- [55] G. J. Ding, S. F. King, X. G. Liu and J. N. Lu, JHEP **1912** (2019) 030 [arXiv:1910.03460 [hep-ph]].
- [56] D. Zhang, Nucl. Phys. B **952** (2020) 114935 [arXiv:1910.07869 [hep-ph]].
- [57] T. Nomura, H. Okada and S. Patra, arXiv:1912.00379 [hep-ph].
- [58] T. Kobayashi, T. Nomura and T. Shimomura, arXiv:1912.00637 [hep-ph].
- [59] J. N. Lu, X. G. Liu and G. J. Ding, arXiv:1912.07573 [hep-ph].
- [60] X. Wang, arXiv:1912.13284 [hep-ph].
- [61] S. J. D. King and S. F. King, arXiv:2002.00969 [hep-ph].
- [62] M. Abbas, arXiv:2002.01929 [hep-ph].
- [63] H. Okada and Y. Shoji, arXiv:2003.11396 [hep-ph].
- [64] H. Okada and Y. Shoji, arXiv:2003.13219 [hep-ph].
- [65] G. J. Ding and F. Feruglio, arXiv:2003.13448 [hep-ph].
- [66] T. Kobayashi, Y. Shimizu, K. Takagi, M. Tanimoto and T. H. Tatsuishi, Phys. Rev. D **100** (2019) no.11, 115045 Erratum: [Phys. Rev. D **101** (2020) no.3, 039904] [arXiv:1909.05139 [hep-ph]].
- [67] H. P. Nilles, S. Ramos-Sanchez and P. K. S. Vaudrevange, arXiv:2004.05200 [hep-ph].
- [68] Z. Maki, M. Nakagawa and S. Sakata, Prog. Theor. Phys. **28** (1962) 870.
- [69] B. Pontecorvo, Sov. Phys. JETP **26** (1968) 984 [Zh. Eksp. Teor. Fiz. **53** (1967) 1717].
- [70] K. Abe *et al.* [T2K Collaboration], Nature **580** (2020) 339.
- [71] P. Adamson *et al.* [NOvA Collaboration], Phys. Rev. Lett. **118** (2017) no.23, 231801 [arXiv:1703.03328 [hep-ex]].
- [72] J. Lauer, J. Mas and H. P. Nilles, Phys. Lett. B **226**, 251 (1989); Nucl. Phys. B **351**, 353 (1991).
- [73] W. Lerche, D. Lust and N. P. Warner, Phys. Lett. B **231**, 417 (1989).
- [74] S. Ferrara, D. Lust and S. Theisen, Phys. Lett. B **233**, 147 (1989).
- [75] D. Cremades, L. E. Ibanez and F. Marchesano, JHEP **0405**, 079 (2004) [hep-th/0404229].

- [76] T. Kobayashi and S. Nagamoto, Phys. Rev. D **96**, no. 9, 096011 (2017) [arXiv:1709.09784 [hep-th]].
- [77] T. Kobayashi, S. Nagamoto, S. Takada, S. Tamba and T. H. Tatsuishi, Phys. Rev. D **97**, no. 11, 116002 (2018) [arXiv:1804.06644 [hep-th]].
- [78] S. Ferrara, D. Lust, A. D. Shapere and S. Theisen, Phys. Lett. B **225**, 363 (1989).
- [79] M. Chen, S. Ramos-Sánchez and M. Ratz, Phys. Lett. B **801** (2020), 135153 [arXiv:1909.06910 [hep-ph]].
- [80] R. C. Gunning, *Lectures on Modular Forms* (Princeton University Press, Princeton, NJ, 1962).
- [81] B. Schoeneberg, *Elliptic Modular Functions* (Springer-Verlag, 1974).
- [82] N. Koblitz, *Introduction to Elliptic Curves and Modular Forms* (Springer-Verlag, 1984).
- [83] S. Antusch and V. Maurer, JHEP **1311** (2013) 115 [arXiv:1306.6879 [hep-ph]].
- [84] F. Björkeröth, F. J. de Anda, I. de Medeiros Varzielas and S. F. King, JHEP **1506** (2015) 141 [arXiv:1503.03306 [hep-ph]].
- [85] M. Tanabashi *et al.* [Particle Data Group], Phys. Rev. D **98** (2018) no.3, 030001.
- [86] T. Kobayashi, Y. Shimizu, K. Takagi, M. Tanimoto, T. H. Tatsuishi and H. Uchida, Phys. Rev. D **101** (2020) no.5, 055046 [arXiv:1910.11553 [hep-ph]].
- [87] I. Esteban, M. C. Gonzalez-Garcia, A. Hernandez-Cabezudo, M. Maltoni and T. Schwetz, JHEP **1901**, 106 (2019) [arXiv:1811.05487 [hep-ph]].
- [88] S. Vagnozzi, E. Giusarma, O. Mena, K. Freese, M. Gerbino, S. Ho and M. Lattanzi, Phys. Rev. D **96** (2017) no.12, 123503 [arXiv:1701.08172 [astro-ph.CO]].
- [89] N. Aghanim *et al.* [Planck Collaboration], arXiv:1807.06209 [astro-ph.CO].
- [90] N. Haba and N. Okamura, Eur. Phys. J. C **14** (2000) 347 [hep-ph/9906481].
- [91] T. Kobayashi and H. Otsuka, arXiv:2004.04518 [hep-th].
- [92] C. Jarlskog, Phys. Rev. Lett. **55** (1985) 1039.
- [93] P. I. Krastev and S. T. Petcov, Phys. Lett. B **205** (1988) 84.